RIP1 inhibition prevents mechanical stress-induced TMJ OA by regulating apoptosis and late-stage necroptosis of chondrocytes

Yiwen Zhou
Department of Orthodontics, Affiliated Stomatological Hospital, Medical School of Nanjing University, Nanjing

Shuang Lin
Department of Orthodontics, Affiliated Stomatological Hospital, Medical School of Nanjing University, Nanjing

Ziwei Huang
Department of Orthodontics, Affiliated Stomatological Hospital, Medical School of Nanjing University, Nanjing

Caixia Zhang
Department of Orthodontics, Affiliated Stomatological Hospital, Medical School of Nanjing University, Nanjing

Huijuan Wang
Department of Orthodontics, Affiliated Stomatological Hospital, Medical School of Nanjing University, Nanjing

Baochao Li
Department of Orthodontics, Affiliated Stomatological Hospital, Medical School of Nanjing University, Nanjing

Huang Li (lihuang76@nju.edu.cn)
Department of Orthodontics, Affiliated Stomatological Hospital, Medical School of Nanjing University, Nanjing

Article

Keywords:

Posted Date: April 11th, 2022

DOI: https://doi.org/10.21203/rs.3.rs-1523906/v1

Abstract

Temporomandibular joint osteoarthritis (TMJ OA) is a common degenerative joint disease that has multiple causes. The abnormal stress distribution is known to be an important trigger of TMJ OA. In order to clarify the mechanism of pathological changes in mandibular cartilage under compressive mechanical stress and the function of RIP1 inhibition through Lenti-virus in mechanical stress-induced TMJ OA, we used a compressive mechanical force-induced-TMJ OA rat model and Lenti-virus targeting RIP1 to perform this study. The results identified the characteristics of the spatio-temporal changes in mechanical stress-induced TMJ OA. Under mechanical force, inflammation and apoptosis, which occur in the whole layer of mandibular cartilage, appear on 4th day and persist till 7th day. Necroptosis arises in the late stage of mechanical force and is mainly located in the transition layer. RIP1 plays an essential role in the destruction of mandibular cartilage under mechanical force. RIP1 inhibition through Lenti-virus could protect mechanical stress-induced mandibular cartilage thinning by inhibiting persisted apoptosis and late-stage necroptosis in the transition layer.

Introduction

Temporomandibular joint osteoarthritis (TMJ OA) is a common degenerative joint disease that has multiple causes. The main pathological changes of TMJ OA are progressive cartilage destruction, chondrocyte death and subchondral bone remodeling. It severely affects patients' daily life by causing joint pain and dysfunction [1]. However, the etiology of TMJ OA is unclear and current treatment has limitations. Non-surgical treatment can only relieve the symptoms[2] but cannot prevent the development of cartilage degeneration. When the disease reaches its final stage, patients are often faced with the only option left for joint surgery[3], which still has a lot of risks[4]. Therefore, it is necessary to further explore the pathogenesis of OA and seek new potential therapeutic targets.

The abnormal stress distribution is known to be an important trigger of TMJ OA[5]. Many studies proved that compressive mechanical stress could induce TMJ OA-like changes[6–12] and we found sixty grams of compressive force could lead to thinning of mandibular cartilage and chondrocytes death.[13] Using our original rat TMJ OA model, we have previously demonstrated that we can reproduce the OA-like pathologic changes after compressive mechanical force loading, allowing investigation of the pathogenesis and new therapeutic target[2,6–10,13–16].

Receptor-interacting protein 1 (RIP1) is a crucial regulator of cell life and death, including a kinase domain, a death domain and an intermediate domain. In the past research, we found RIP1 and TNF-α were increased in the mandibular cartilage under compressive mechanical stress. It indicates that compressive stress can regulate the expression of RIP1, but it is unknown whether RIP1 plays a role in TMJ OA development. On the other hand, it is reported that RIP1 is a key upstream regulator which mediates many signaling pathways, including RIP1/RIP3-mediated necroptosis[16,17], TRADD-dependent

apoptosis[18] and NF-κB-related inflammation[19,20]. Targeting RIP1 might be a novel therapeutic strategy for different diseases including TMJ OA[19].

In the present study, we hypothesized that RIP1 inhibition can block necroptosis, apoptosis and inflammatory signaling pathways in a special spatio-temporal pattern, and protect TMJ from compressive mechanical stress stimulation. By injecting Lenti-virus-mediated-siRNA targeting RIP1 (Lenti-siRIP1) into TMJ, the expression of RIP1 was inhibited in mandibular chondrocytes and the histological changes of TMJ were measured. The expression of necroptosis, apoptosis and inflammatory factors were investigated. The research should discover the mechanism of RIP1 during the progress of TMJ-OA and provide a new therapeutic target of TMJ OA.

Results

1. Lenti-siRIP1 successfully inhibits compressive mechanical force-induced RIP1 expression in vivo

To explore the role of RIP1 in mechanical force-induced TMJ OA, we used our original TMJ OA rat model[6–10, 13,15,16] with the intra-articular injection of Lenti-siRIP1 to mediate RIP1 knockdown (Fig. 1). After loading compressive mechanical force for 4 or 7 days, RIP1 mRNA was significantly increased and the increase was more obvious in the 4 d group (3.69-fold in the 4 d group and 2.2-fold in the 7 d group, P 0.01). With the injection of Lenti-siRIP1, the mRNA level of RIP1 was significantly decreased compared to the F groups (50.9% in the 4 d group and 39.8% in the 7 d group, P 0.01). Also, the protein level of RIP1 declined (37.1% in the 4 d group and 34.9% in the 7 d group by Immunohistochemistry, P 0.01). In both 4 d and 7 d, the decrease was more obvious in proliferative and hypertrophic layers. Considering the low expression of RIP1 in mandibular cartilage, the siRIP1-only group did not reveal a statistical difference compared with Con groups. Thus, the rise of RIP1 in mandibular cartilage under mechanical force could be inhibited by the injection of Lenti-siRIP1.

2. RIP1 inhibition protects mandibular cartilage thinning under compressive mechanical force stimulation

During the progress of compressive mechanical stress-induced TMJ OA, destruction of mandibular cartilage is an obvious pathological change, including the change of cell morphology, cell number, and cartilage thickness. Therefore, we performed H&E staining to detect the change of cartilage to test whether Lenti-siRIP1 had a protective effect on mandibular cartilage.

In the F group, cartilage damage increased time-dependently, showing apparent thinning and chondrocyte loss (Fig. 2). Chondrocytes under mechanical force shrunk in size, arranged irregularly and flattened. The number of chondrocytes also decreased (20.2% in the 4 d group and 29.0% in the 7 d group, P 0.01). Consistent with the cell number, the thickness of mandibular cartilage became thinning (25.7% in 4 d group and 39.8% in 7 d group, P 0.01). Interestingly, by measuring the thickness of different layers, we found that in the 4 d group, the thickness of the hypertrophic layer decreased more obviously (32.4% in

the 4 d group's hypertrophic layer, P 0.01). While in the 7 d group, the proliferative layer showed more thinning (46.8% in the 7 d group's proliferative layer, P 0.01).

In the F + siRIP1 group, the thickness of mandibular cartilage recovered (31.8% in the 4 d group and 35.0% in the 7 d group, P 0.01) and the number of chondrocytes raised (22.8% in the 4 d group and 23.4% in the 7 d group, P 0.01) compared with the F group. In the 4 d group, hypertrophic layers' thickness recovered most obviously (56.5% in the 4 d group and 43.3% in the 7 d group, P 0.01). This demonstrated that Lenti-siRIP1 significantly relieves mandibular cartilage thinning under compressive mechanical force.

3. RIP1 inhibition decreases the mortality of chondrocytes under compressive mechanical force

To further investigate the protective efficiency of Lenti-siRIP1 among chondrocytes, we used TUNEL staining to observe dead cells. Without mechanical force, there was nearly no dead cell in mandibular cartilage. After loading force, dead chondrocytes occurred and showed a time-dependent increasing trend (Fig. 3). The distribution of dead cells also has certain characteristics. In the 4 d group, dead cells were mainly distributed in the transition layer and the hypertrophic layer, while in the 7 d group, dead chondrocytes were scattered throughout the whole layer of mandibular cartilage.

RIP1 inhibition rescued the death of chondrocytes under compressive mechanical force in both 4 d (30.4%, P 0.01) and 7 d (36.0%, P 0.01) groups, strongly demonstrating the therapeutic effectiveness. Chondrocytes' death in proliferative, transition and hypertrophic layers were all alleviated by Lenti-siRIP1, showing that Lenti-virus transfection had effects on the whole layer of mandibular cartilage. Among this, the transition layer recovered most in the 4 d group (37.3%, P 0.01) while the proliferative layer recovered most in the 7 d group (50.7%, P 0.01).

4. RIP1 inhibition in mandibular cartilage could not protect subchondral bone under compressive mechanical force

Another pathological change during stress-induced TMJ OA is the destruction and remodeling of subchondral bone. Consistent with our previous study (Fig. 4), at the early stage (4 d), subchondral bone showed decreased percent bone volume (BV/TV), indicating the loss of bone mass. Bone trabecula which supports subchondral bone plate also showed damage, including decreased trabecular number (Tb.N), trabecular thickness (Tb.Th) and increased trabecular separation (Tb.Sp). After loading mechanical force for 7 days, the destruction remained but recovered a little, indicating the initiation of bone remodeling under compressive mechanical stress.

Nonetheless, there was no significant difference between the F + siRIP1 group and the F group on both 4 d and 7 d. The loss of bone mass remained and bone trabecula still showed diffuse microdamage. Meanwhile, in the 7 d group, there was no signal of earlier bone remodeling due to Lenti-siRIP1. Thus,

RIP1 inhibition in mandibular cartilage by injecting Lenti-siRIP1 into TMJ could not protect subchondral bone under mechanical force.

5. RIP1 inhibition reduces the mechanical stress-induced expression of inflammatory factors in the cartilage

After confirming the protective role of Lenti-siRIP1 in mandibular cartilage under mechanical force, we further determined the underlying mechanism. As for inflammatory markers, TNF-α and IL-1β both increased in the F group compared with the Con group, indicating the activation of inflammation in the mandibular cartilage during the whole process of force application (Fig. 5). The mRNA level of TNF-α rose rapidly in the 4 d group (5.8-fold, P 0.01) while the protein level also showed increase in the F group (2.1-fold in the 4 d group and 3.9-fold in the 7 d group, P 0.01). IL-1β increased obviously on 4 d (1.9-fold in mRNA and 3.4-fold in protein, P 0.01). While in the 7 d group, the mRNA level of IL-1β had no significant difference compared with the Con group (1.2-fold, P 0.05) but the protein level was higher (2.5-fold, P 0.01). TNF-α was mainly located in the proliferation and transition layers while IL-1β was more expressed in the transition and hypertrophic layers.

Lenti-siRIP1 prevented the increase of TNF-α and IL-1β on both 4 d and 7 d, suggesting the inhibition of stress-induced inflammation in mandibular cartilage. In the F + siRIP1 group, TNF-α decreased both at the mRNA (51.7% in the 4 d group and 32.0% in the 7 d group, P 0.01) and protein (28.0% in the 4 d group and 43.5% in the 7 d group, P 0.01) levels. The expression of IL-1β also declined both at the mRNA (58.8% in the 4 d group and 65.8% in the 7 d group, P 0.01) and protein (55.3% in the 4 d group and 44.6% in the 7 d group, P 0.01) levels. The decrease of inflammatory factors appeared in all layers, suggesting the function of Lenti-siRIP1 could penetrate mandibular cartilage and alleviate inflammation induced by compressive mechanical force.

6. RIP1 inhibition reduces the mechanical stress-induced apoptosis and late-stage necroptosis of chondrocytes

TUNEL staining (Fig. 3) revealed that a large number of chondrocytes died after loading mechanical force. In order to clarify the form of cell death, we further detected the expression of Caspase-8 and RIP3, which represent apoptosis and necroptosis respectively (Fig. 6).

After loading mechanical force for 4 d, the expression level of Caspase-8 in mandibular cartilage showed an obvious upward trend compared with the Conrol group (2.1-fold in mRNA and 6.4-fold in protein, P 0.01), indicating the activation of apoptosis at the early stage. In the 7 d F group, the level of Caspase-8 was still higher than the Con group (1.4-fold in mRNA and 3.53-fold in protein, P 0.01), but lower than the 4 d F group, suggesting that apoptosis was reduced but still remained under 7 days' mechanical force. Different from the early high expression of Caspase-8, RIP3 did not show any increase in the 4 d F group, suggesting that in the early stage of stress-induced TMJ OA, necroptosis did not appear in mandibular cartilage. On 7 d, the expression of RIP3 increased (1.5-fold in mRNA and 2.0-fold in protein, P 0.01).

Combined with the decrease of Caspase-8 on 7 d, it represented that necroptosis was activated in chondrocytes at the later stage of stress-induced TMJ OA. Under mechanical stress, Caspase-8 could be found in all layers, especially in the hypertrophic layer, whereas RIP3 was mainly found in the transition layer.

Compared with the F group, Caspase-8 in the F + siRIP1 group decreased both at the mRNA (49.3% on 4d and 36.2% on 7d, P 0.01) and protein (62.8% on 4d and 25.4% on 7d, P 0.01) levels, indicating the inhibition of apoptosis during the whole progress. In the 7 d group, RIP3 decreased obviously (65.5% in mRNA and 25.9% in protein, P 0.01) in the F + siRIP1 group, demonstrating the effectiveness of Lenti-siRIP1 in preventing the necroptosis. Therefore, as an important upstream regulator, RIP1 inhibition could protect mandibular cartilage in stress-induced TMJ OA by alleviating persisted apoptosis and late-stage necroptosis.

Discussion

In our previous study, we found RIP1 increased obviously during chondrocyte death under compressive mechanical force[15]. Therefore, the function of RIP1 in stress-mediated TMJ OA awakened our interest. RIP1 is an important upstream kinase, crucial to cell survival and mediating cell death through different pathways[21]. In the present study, we chose Lenti-virus injection to explore the protective effect of RIP1 inhibition on mandibular cartilage under compressive mechanical stress. The results showed that RIP1 inhibition by injecting Lenti-siRIP1 could effectively protect mandibular cartilage under compressive mechanical stress. The thickness of mandibular cartilage was recovered and chondrocyte death was alleviated. Inflammation, apoptosis and necroptosis induced by compressive mechanical stress were all inhibited. Targeting RIP1 is a feasible therapeutic strategy for stress-induced TMJ OA.

The function of RIP1 is complex. In our study, inflammation and apoptosis occurred at the early stage and persisted till the end with the increase of TNF-α, IL-1β, RIP1 and Caspase-8, while necroptosis appeared at the later stage with the increase of RIP3. RIP1 could suppress apoptosis and necroptosis through NF-κB pathway[22]. Lacking RIP1 in mice leads to death soon after birth[23].Furthermore, mice conditional knockout RIP1 experience inflammation, RIP3/MLKL-dependent necroptosis and Caspase-8-dependent apoptosis and die in early age[24], which was in lined with our results. After TNF-α binding to TNFR1, TNF-receptor-associated death domain (TRADD) recruits RIP1 and then forms the complex I. Meanwhile, complex I can transform into the death-inducing complex IIa/b after Caspase-8 activation and induce apoptosis[25]. When Caspase-8 is inhibited, RIP1 and RIP3 are combined to form complex IIc (the necrosome), which can induce necroptosis[17,26]. Our results confirmed that RIP1 plays different roles during different pathological stages in stress-induced TMJ OA. At the early stage, RIP1 and Caspase-8 increased significantly, indicating the activation of Caspase-8 dependent apoptosis. After loading mechanical force for 7 d, while the expression of RIP3 increased, Caspase-8 went down but still higher than the control, suggesting that necroptosis was activated and apoptosis persisted. With the activation of necroptosis, cellular contents are released to inactivate immune cells and further promote

inflammation by generating TNF-α to stimulate RIP1, [27], which showed continue existing inflammation. In summary, inflammation and apoptosis persist in the destruction of mandibular cartilage under compressive mechanical stress, but necroptosis appears on the late stage in the present study.

Unfortunately, we also found RIP1 inhibition in condylar cartilage could not protect subchondral bone's destruction. Although it is reported that RIP1/RIP3 pathway plays an essential role in the differentiation of osteoclast and restraining RIP1 could hinder osteoclastogenesis and attenuate bone loss[28], our result showed the transfection of Lenti-siRIP1 mainly focused on the cartilage layer, and hard to transfect and penetrate subchondral bone.

To sum up, in our rat model of stress-induced TMJ OA, RIP1 was increased significantly in condylar cartilage, accompanied by the elevation of inflammatory, apoptotic and necroptotic factors including TNF-α, IL-1β, Caspase-8 and RIP3. The inhibition of RIP1 showed spatio-temporal protective effects on mandibular cartilage under compressive mechanical force. The RIP1 inhibition could protect chondrocytes by restraining inflammation, apoptosis and late-stage necroptosis. The study demonstrated the therapeutic potential of Lenti-virus targeting RIP1 in stress-induced TMJ OA.

Conclusion

Our study identified RIP1 plays an essential role in the destruction of mandibular cartilage under the mechanical force. RIP1 inhibition through Lenti-virus could protect mechanical stress-induced mandibular cartilage thinning by inhibiting inflammation, apoptosis and necroptosis spatio-temporal changes.

Materials And Methods

Animal Experiments

All animal experiments were performed with the regulation and approval by the Animal Ethics Committee of Nanjing University Medical School (Protocol Number: IACUC-D2202073) and complied with the ARRIVE (Animal Research: Reporting in Vivo Experiments) guidelines for preclinical animal studies. All surgery was performed under sodium pentobarbital anesthesia, and all efforts were made to minimize suffering. A total of 240 (the power calculated by PASS 11.0 software was more than 80%) 7-week-old male Sprague Dawley rats weighing 180-200g were requisitioned in this study. Rats were divided into two groups randomly: Control group(Con group)and Force group（F group）.

For rats in the F group, 60 g compressive mechanical force was applied on the first day of the experiment: Two stainless steel hooks were fixed on the lower incisors of the rats by resin. An anchorage jig was placed around the neck and arms. Between the hooks and jig, two rubber bands were tied on both sides, loading 60 g mechanical force up and backward. The rubbers were changed every 3 days to maintain stable force (Supplementary Fig. 1). When the compressive mechanical stress was applied, Lenti-shRNA (negative Lenti-virus) was injected locally into the right TMJ and Lenti-siRIP1 was injected into the left

TMJ in both Con and F groups. Each rat was injected once throughout the entire experiment. On the 4th day (4 d) and 7th day (7 d) after mechanical force loading, rats were sacrificed for subsequent experiments.

Preparation of Mandibular chondrocytes

The mandibular chondrocytes were isolated from 3-week-old Sprague Dawley male rats to investigate the optimal transfection conditions. In brief, after separating soft tissues of the mandibular condyle, condylar cartilage was carefully dissected and digested with 0.25% trypsin for 30 min and 0.2% collagenase for 3 h. The suspension was filtrated and centrifuged so that chondrocytes were isolated as single cells. Then, primary chondrocytes were seeded at $1\times10^5/cm^2$ density and cultured with DMEM complete medium in a humidified atmosphere at 37°C with 5% CO2. The medium was replaced every 2 days and the cells were passaged when the fusion reached 90%. The third generation was used for *in-vitro* transfection.

Preparation of Lenti-virus and transfection

3 pairs of small interfering RNA (siRNA) targeting RIP1 were designed and correspondent Lenti-viruses were constructed by Novobio Scientific Co. LTD. (Shanghai, China). By *in-vitro* experiments, Lenti-virus with optimal siRNA sequence (top strand:5'-CACCGCAGTTCTTGGTCTGCATAAACGAATTTATGCAGACCAAGAACTGC-3', bottom strand:5'-AAAAGCAGTTCTTGGTCTGCATAAATTCGTTTATGCAGACCAAGAACTGC-3') was chosen as Lenti-siRIP1 for subsequent i*n-vivo* experiments (Supplementary Fig. 2). For each side of TMJ, 20μl hybrid liquid including 5μg/ml Polybrene and $2x10^8$Tu/ml Lenti-virus was injected.

Isolation of total RNA and Analysis

Three mandibular cartilages from three different rats in the same group were considered as one sample for RNA extraction. Total RNA was extracted from cartilage by RNA extraction kit (Tianenze, Beijing, China) according to the manufacturer's instructions and was reversed into cDNA. The primers used are listed in Supplementary Table 1. All genes were analyzed by quantitative real-time PCR (Biosystems 7500 real-time PCR machine) and expressions were normalized by GAPDH. Each experiment was performed 3 times and average values were calculated as means.

Isolation of total protein and Western Blot

The mandibular cartilage was cut into pieces and lysed with RIPA and PMSF (RIPA: PMSF = 100: 1) buffer to obtain total protein. Quantified by the Bradford method, 25μg of total protein was loaded and isolated via 12% SDS-PAGE Gel. After protein was transferred onto PVDF membrane, the antibody of RIP1 (1:500, NBP1-77077, Novusbio, UK) and beta-action (1:1000, ab8226, Abcam, UK) were incubated overnight, followed by incubation of Goat anti-Rabbit HRP-conjugated secondary mAbs (1:5000, ab6721, Abcam, UK) for 1 h. The membrane was visualized using an ECL Plus Kit (Amersham Biosciences, Amersham, Bucks, UK) and quantified by densitometry (ImageJ 1.8.0).

Histological observation and histomorphometric measurements

After 4 or 7 days, the rats were sacrificed and mandibular condyles were isolated with the surrounding tissue. Samples were fixed in paraformaldehyde for 24h and decalcified in a 15% ethylenediaminetetraacetic acid (EDTA) solution for 8 weeks. After paraffin embedding, 5-um-thick sagittal sections were cut from each TMJ block parallel to the lateral surface of the condylar neck of the mandible ramus. Sections were dewaxed with xylene and rehydrated in a graded alcohol series for hematoxylin and eosin staining. Images were captured with an Olympus XI 70 microscope equipped with an Olympus Magna Fire digital camera. The mandibular cartilage thickness was measured on three HE-stained sections per joint by a computer-assisted image analysis system (Image-Pro Plus, 6.0) at the same staining threshold and the average values were taken for statistical analysis.

Immunohistochemical staining

Sections were treated with 3% hydrogen peroxide to eliminate endogenous peroxidase activity and digested the antigenic sites with Antigen Retrieval Solution (AR0026, Wuhan Boster Biological Technology Ltd. China) for 10 min. Antibodies of RIP1 (1: 100, NB1-77077, Novusbio, UK),TNF-α (1: 1000, ab66579, Abcam, UK), IL-1β (1: 100, ab9787, Abcam, UK), RIP3 (1: 100, ab58828, Abcam, UK) and Caspase-8 (1: 100, ab25901, Abcam, UK) were incubated overnight at 4℃.Then, the specimens were incubated with biotin-labeled IgG (GB23404, Servicebio, Wuhan, China) for 30min at 37℃ and an avidin-peroxidase complex for 30min at 37℃. Antibodies in the specimens were stained by a peroxidase/diaminobenzidine (DAB) yellow kit (AR1000, Wuhan Boster Biological Technology Ltd. China). Sections were also stained with hematoxylin, dehydrated in an ethanol series, cleared in xylene and covered slips. Image acquisition was the same as described above. The color difference marking positive and negative areas was measured with Image-Pro Plus and scores were assessed according to the staining intensity.

TUNEL staining

5-um-thick sections of mandibular cartilages were prepared and apoptotic cells were stained using TUNEL cell apoptotic kits (MK1027, Wuhan Boster Biological Technology Ltd. China) according to the manufacturer's protocol. The percentage of apoptotic cells was measured with Image-Pro Plus (3 sections per specimen, 6 specimens in each group).

Micro-computed tomography

Tissues containing mandibular condyles were fixed in 4% paraformaldehyde solution. The morphology of condyles was assessed using an animal micro-CT scanner (GE eXplore Locus SP, London). The specimens were scanned with some parameters, including an X-ray tube potential of 80 kV, a tube current of 0.45mA and 9-um voxel resolution. After the micro-CT scan, the visualization of subchondral bone was made with software (Health Care MicroView ABA 2.1.2). Micro-CT measurements included percent bone

volume (BV/TV), trabecular number (Tb.N), trabecular thickness (Tb.Th) and trabecular separation (Tb.sp) in the bone defect.

Statistical analysis

All measurements were repeated three times. All statistical calculations were performed using SPSS version 13.0 statistical software. The data were expressed as means ± SD and one-way ANOVA was used to determine statistical significance between groups. P□0.05 was considered statistically significant. The datasets analysed during the current study are available in the Mendeley Data (DOI: 10.17632/hw229v7p2k.1).

Declarations

Acknowledgments

This research was supported by the National Natural Science Foundation of China (grant numbers: 81670960), Natural Science Foundation of Jiangsu(grant numbers: SBK2021021787) and Nanjing key project Foundation (grant numbers: ZKX20048). The authors declare no potential conflicts of interest with respect to authorship and the publication of this article.

Author contributions

Yiwen Zhou and Shuang Lin contributed to data acquisition, analysis and drafted the manuscript. Ziwei Huang and Caixia Zhang contributed to *in vivo* experiments and revised the manuscript. Huijuan Wang and Baochao Li contributed to *in vitro* experiments. Huang Li conceived of and designed the study and revised the manuscript.

Conflict of interest

We declare that we have no conflict of interest.

Competing interests

The authors declare no competing interests.

References

1. Kapos, F. P., Exposto, F. G., Oyarzo, J. F. & Durham, J. Temporomandibular disorders: a review of current concepts in aetiology, diagnosis and management. Oral Surg **13**, 321–334, doi:10.1111/ors.12473 (2020).

2. Andre, A., Kang, J. & Dym, H. Pharmacologic Treatment for Temporomandibular and Temporomandibular Joint Disorders. Oral Maxillofac Surg Clin North Am **34**, 49–59, doi:10.1016/j.coms.2021.08.001 (2022).
3. Asquini, G., Pitance, L., Michelotti, A. & Falla, D. The effectiveness of manual therapy applied to craniomandibular structures in temporomandibular disorders: a systematic review. J Oral Rehabil, doi:10.1111/joor.13299 (2021).
4. Bach, E., Sigaux, N., Fauvernier, M. & Cousin, A. S. Reasons for failure of total temporomandibular joint replacement: a systematic review and meta-analysis. Int J Oral Maxillofac Surg, doi:10.1016/j.ijom.2021.12.012 (2022).
5. Betti, B. F. *et al.* Effect of mechanical loading on the metabolic activity of cells in the temporomandibular joint: a systematic review. Clin Oral Investig **22**, 57–67, doi:10.1007/s00784-017-2189-9 (2018).
6. Huang, Z. *et al.* BRD4 inhibition alleviates mechanical stress-induced TMJ OA-like pathological changes and attenuates TREM1-mediated inflammatory response. Clin Epigenetics **13**, 10, doi:10.1186/s13148-021-01008-6 (2021).
7. Jiang, Y. Y. *et al.* BIO alleviated compressive mechanical force-mediated mandibular cartilage pathological changes through Wnt/beta-catenin signaling activation. J Orthop Res **36**, 1228–1237, doi:10.1002/jor.23748 (2018).
8. Wen, J., Jiang, Y., Zhang, C., Chen, S. & Li, H. The Protective Effects of Salubrinal on the Cartilage and Subchondral Bone of the Temporomandibular Joint under Various Compressive Mechanical Stimulations. PLoS One **11**, e0155514, doi:10.1371/journal.pone.0155514 (2016).
9. Zhang, C., Xu, Y., Cheng, Y., Wu, T. & Li, H. Effect of asymmetric force on the condylar cartilage, subchondral bone and collagens in the temporomandibular joints. Arch Oral Biol **60**, 650–663, doi:10.1016/j.archoralbio.2015.01.008 (2015).
10. Zhang, C. *et al.* LOXL2 attenuates osteoarthritis through inactivating Integrin/FAK signaling. Sci Rep **11**, 17020, doi:10.1038/s41598-021-96348-x (2021).
11. Ikeda, Y., Yonemitsu, I., Takei, M., Shibata, S. & Ono, T. Mechanical loading leads to osteoarthritis-like changes in the hypofunctional temporomandibular joint in rats. Arch Oral Biol **59**, 1368–1376, doi:10.1016/j.archoralbio.2014.08.010 (2014).
12. Li, W. *et al.* Role of HIF-2α/NF-κB pathway in mechanical stress-induced temporomandibular joint osteoarthritis. Oral Dis, doi:10.1111/odi.13986 (2021).
13. Li, H. *et al.* Endoplasmic reticulum stress regulates rat mandibular cartilage thinning under compressive mechanical stress. J Biol Chem **288**, 18172–18183, doi:10.1074/jbc.M112.407296 (2013).
14. Li, H. *et al.* Proteomic analysis of early-response to mechanical stress in neonatal rat mandibular condylar chondrocytes. J Cell Physiol **223**, 610–622, doi:10.1002/jcp.22052 (2010).
15. Zhang, C. *et al.* Mechanical force-mediated pathological cartilage thinning is regulated by necroptosis and apoptosis. Osteoarthritis Cartilage **25**, 1324–1334, doi:10.1016/j.joca.2017.03.018

(2017).

16. Zhang, Y. *et al.* RIP1 autophosphorylation is promoted by mitochondrial ROS and is essential for RIP3 recruitment into necrosome. Nat Commun **8**, 14329, doi:10.1038/ncomms14329 (2017).
17. Liu, Y. *et al.* RIP1/RIP3-regulated necroptosis as a target for multifaceted disease therapy (Review). Int J Mol Med **44**, 771–786, doi:10.3892/ijmm.2019.4244 (2019).
18. Li, X. *et al.* RIP1-dependent linear and nonlinear recruitments of caspase-8 and RIP3 respectively to necrosome specify distinct cell death outcomes. Protein Cell **12**, 858–876, doi:10.1007/s13238-020-00810-x (2021).
19. Ofengeim, D. & Yuan, J. Regulation of RIP1 kinase signalling at the crossroads of inflammation and cell death. Nat Rev Mol Cell Biol **14**, 727–736, doi:10.1038/nrm3683 (2013).
20. Patel, S. *et al.* RIP1 inhibition blocks inflammatory diseases but not tumor growth or metastases. Cell Death Differ **27**, 161–175, doi:10.1038/s41418-019-0347-0 (2020).
21. Newton, K. & Manning, G. Necroptosis and Inflammation. Annu Rev Biochem **85**, 743–763, doi:10.1146/annurev-biochem-060815-014830 (2016).
22. Vanlangenakker, N., Bertrand, M. J., Bogaert, P., Vandenabeele, P. & Vanden Berghe, T. TNF-induced necroptosis in L929 cells is tightly regulated by multiple TNFR1 complex I and II members. Cell Death Dis **2**, e230, doi:10.1038/cddis.2011.111 (2011).
23. Kelliher, M. A. *et al.* The death domain kinase RIP mediates the TNF-induced NF-kappaB signal. Immunity **8**, 297–303, doi:10.1016/s1074-7613(00)80535-x (1998).
24. Rickard, J. A. *et al.* RIPK1 regulates RIPK3-MLKL-driven systemic inflammation and emergency hematopoiesis. Cell **157**, 1175–1188, doi:10.1016/j.cell.2014.04.019 (2014).
25. Micheau, O. & Tschopp, J. Induction of TNF receptor I-mediated apoptosis via two sequential signaling complexes. Cell **114**, 181–190, doi:10.1016/s0092-8674(03)00521-x (2003).
26. Wang, H. *et al.* Mixed lineage kinase domain-like protein MLKL causes necrotic membrane disruption upon phosphorylation by RIP3. Mol Cell **54**, 133–146, doi:10.1016/j.molcel.2014.03.003 (2014).
27. Li, J. *et al.* The RIP1/RIP3 necrosome forms a functional amyloid signaling complex required for programmed necrosis. Cell **150**, 339–350, doi:10.1016/j.cell.2012.06.019 (2012).
28. Liang, S., Nian, Z. & Shi, K. Inhibition of RIPK1/RIPK3 ameliorates osteoclastogenesis through regulating NLRP3-dependent NF-κB and MAPKs signaling pathways. Biochem Biophys Res Commun **526**, 1028–1035, doi:10.1016/j.bbrc.2020.03.177 (2020).

Figures

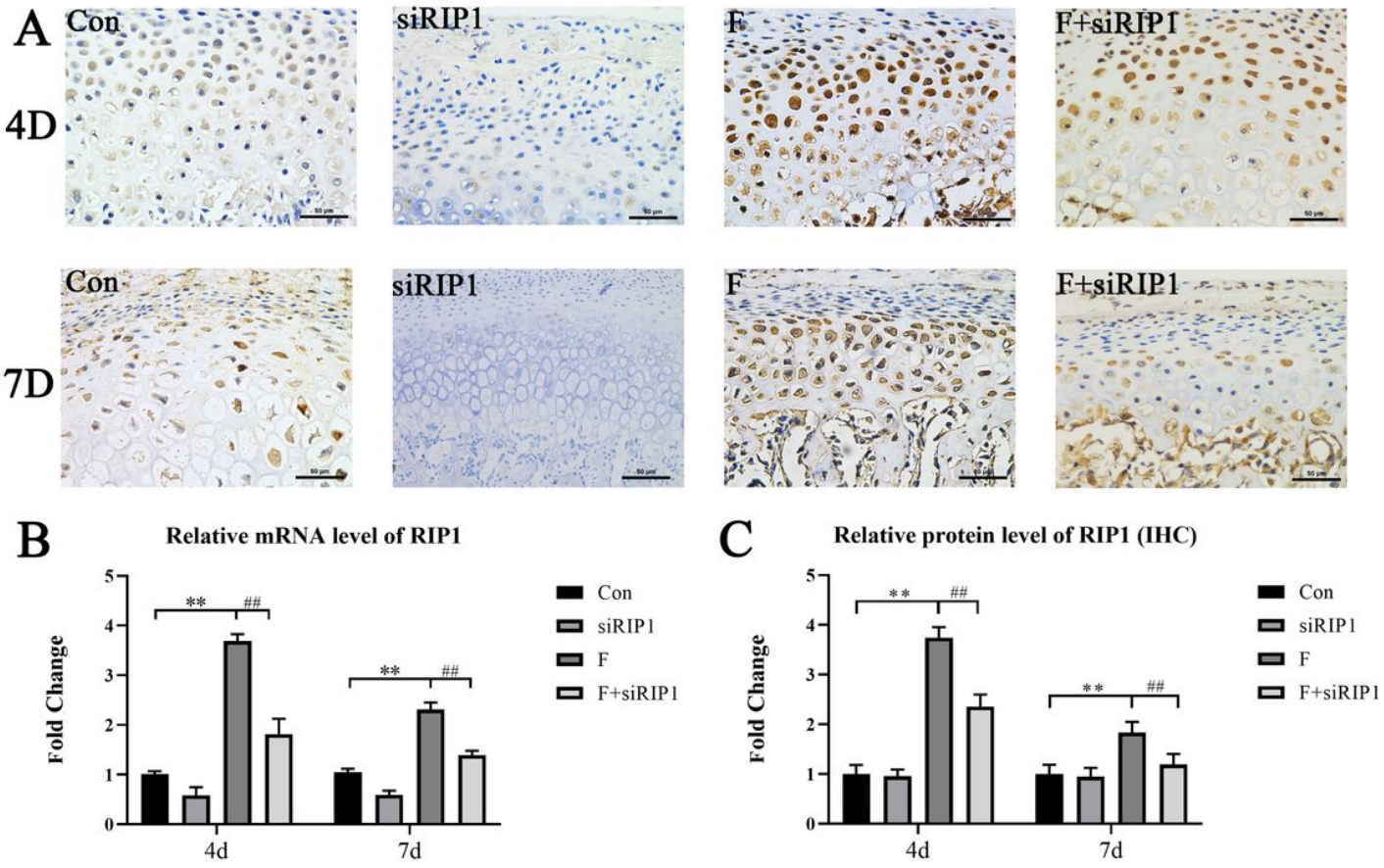

Figure 1

RIP1 expression in mandibular cartilage was decreased by Lenti-siRIP1.

Lenti-virus-constructed short hairpin RNA (Lenti-shRNA) or Lenti-siRIP1 was transfected into mandibular cartilage. Tissues from Con (Lenti-shRNA), siRIP1 (Lenti-siRIP1), F (Force+Lenti-shRNA) and F+siRIP1 (Force+Lenti-siRIP1) groups were collected for analysis of relative RIP1 levels. **(a&c)** Immunohistochemical analysis of RIP1 in condylar cartilage at 4 d and 7 d (n=6). Scale bar indicates 50 μm. **(b)** Quantitative real-time PCR analysis of RIP1 in condylar cartilage at 4 d and 7 d (n=6). Data were normalized based on GAPDH and were expressed as mean ± SD. (**P*＜0.05 vs Con group; ***P*＜0.01 vs Con group; #*P*＜0.05 vs F group; ##*P*＜0.01 vs F group)

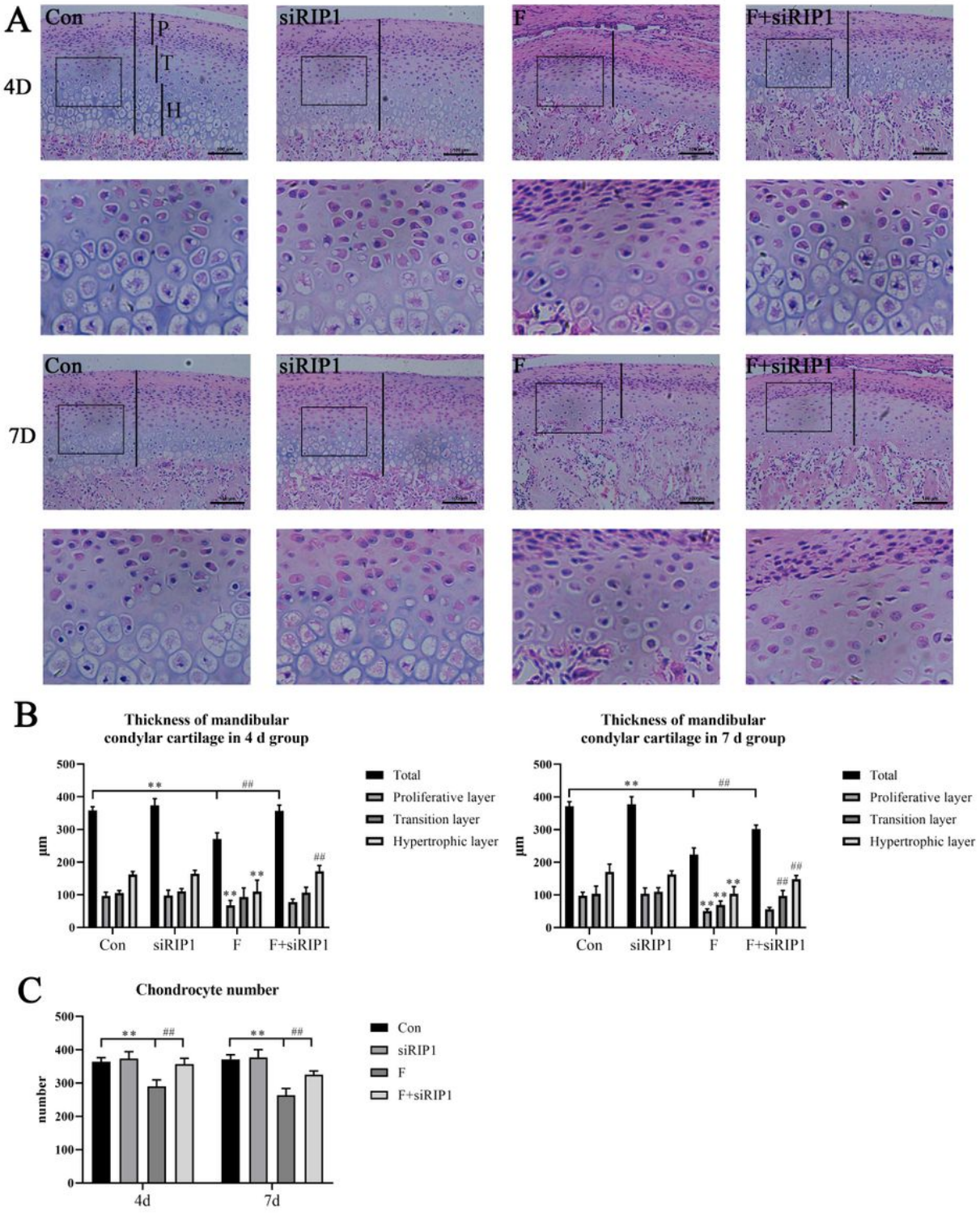

Figure 2

Mandibular cartilage destruction under compressive mechanical force was protected by Lenti-siRIP1.

(a) Haematoxylin and eosin (H&E) staining of mandibular cartilage from Con, siRIP1, F and F+siRIP1 groups (n=6). The lines represent the measurement of cartilage thickness and figures in the boxes are amplified to show clear histological change. P indicates proliferative zone, T indicates transition zone,

and H indicates hypertrophic zone. Scale bar indicates 50 μm. **(b)** The measurement of cartilage thickness in each group (n=6). **(c)** The measurement of chondrocyte number in each group (n=6). Data were expressed as mean ± SD. (*P<0.05 vs Con group; **P<0.01 vs Con group; #P<0.05 vs F group; ##P<0.01 vs F group)

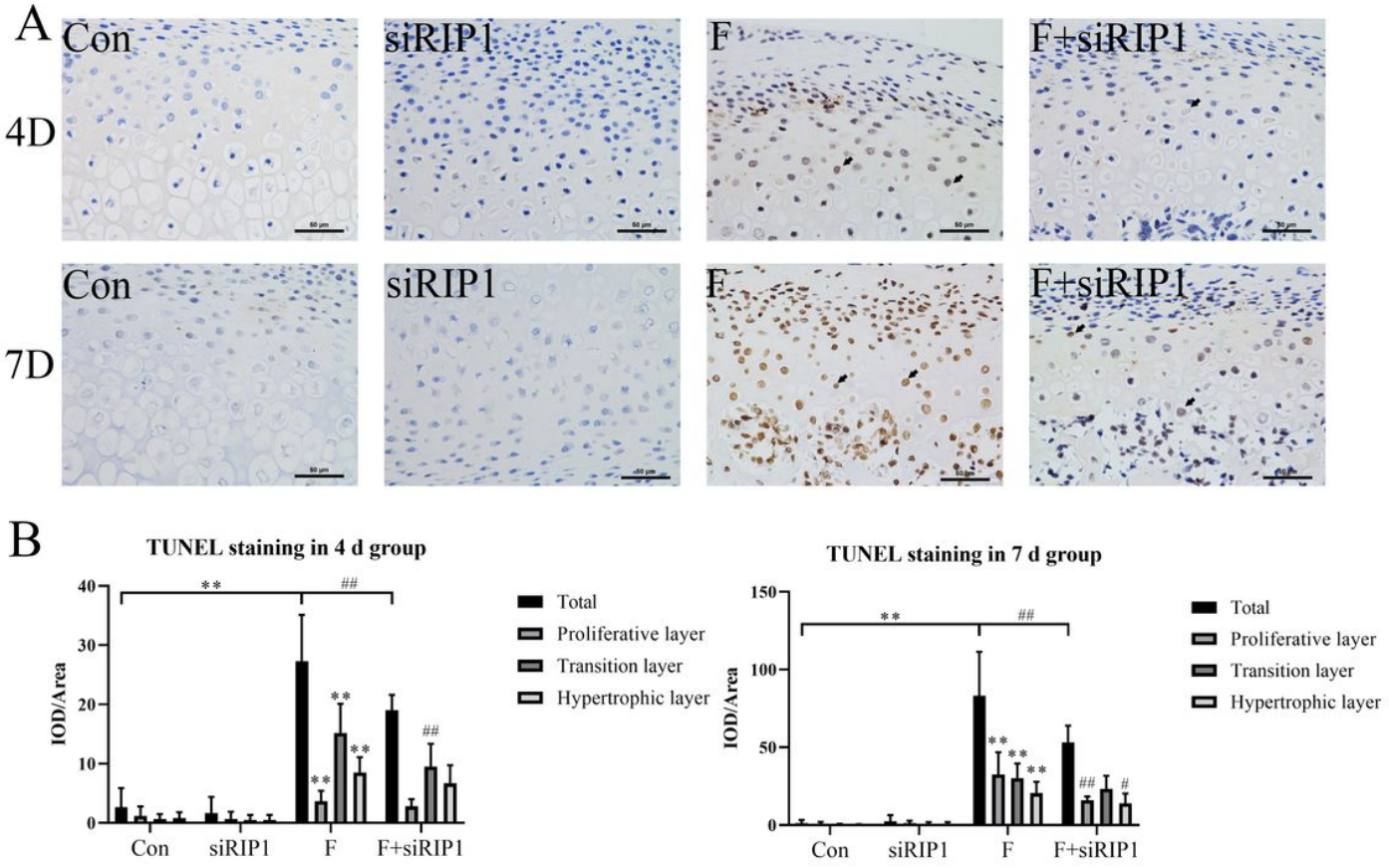

Figure 3

The death rate of chondrocytes under mechanical force decreases after injecting Lenti-siRIP1.

(a) Condyle sections from Con, siRIP1, F and F+siRIP1 groups were subjected to TUNEL staining to observe dead cells (n=6). The black arrows indicate representative dead chondrocytes. Scale bar indicates 50 μm. **(b)** Quantification of TUNEL staining. Proliferation zone, transition zone and hypertrophic zone are the same as described in Figure 2. Data were expressed as mean ± SD. (*P<0.05 vs Con group; **P<0.01 vs Con group; #P<0.05 vs F group; ##P<0.01 vs F group)

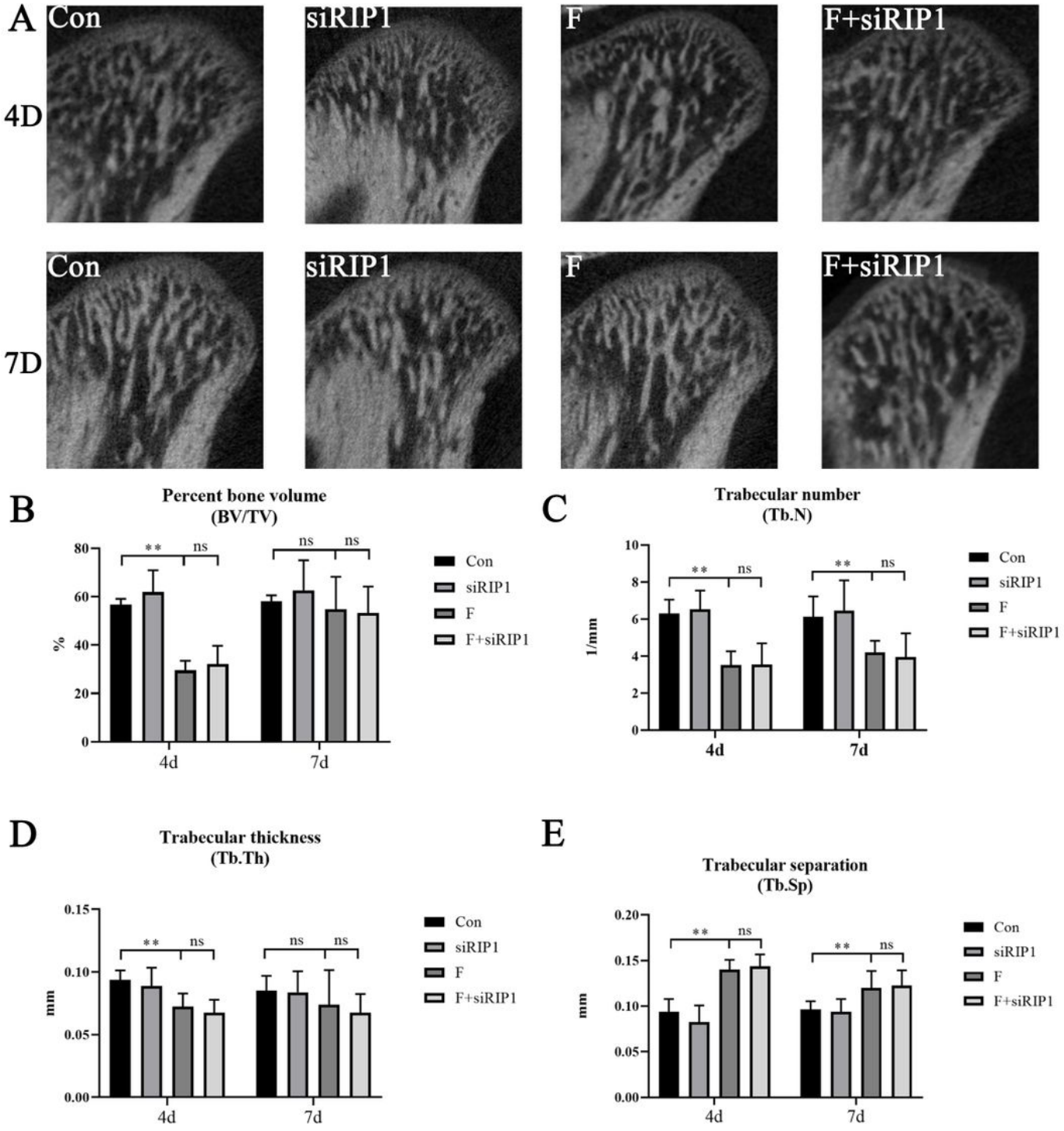

Figure 4

Destruction of subchondral bone was not prevented by Lenti-siRIP1.

(a) Micro-computed tomography (Micro-CT) reconstructed images of condyles in Con, siRIP1, F and F+siRIP1 groups (n=8). **(b-e)** Exhibitions of quantitative parameters include percent bone volume (BV/TV),

trabecular number (Tb.N), trabecular thickness (Tb.Th) and trabecular separation (Tb.sp). Data were expressed as mean ± SD. (**P 0.01, ns=no significant)

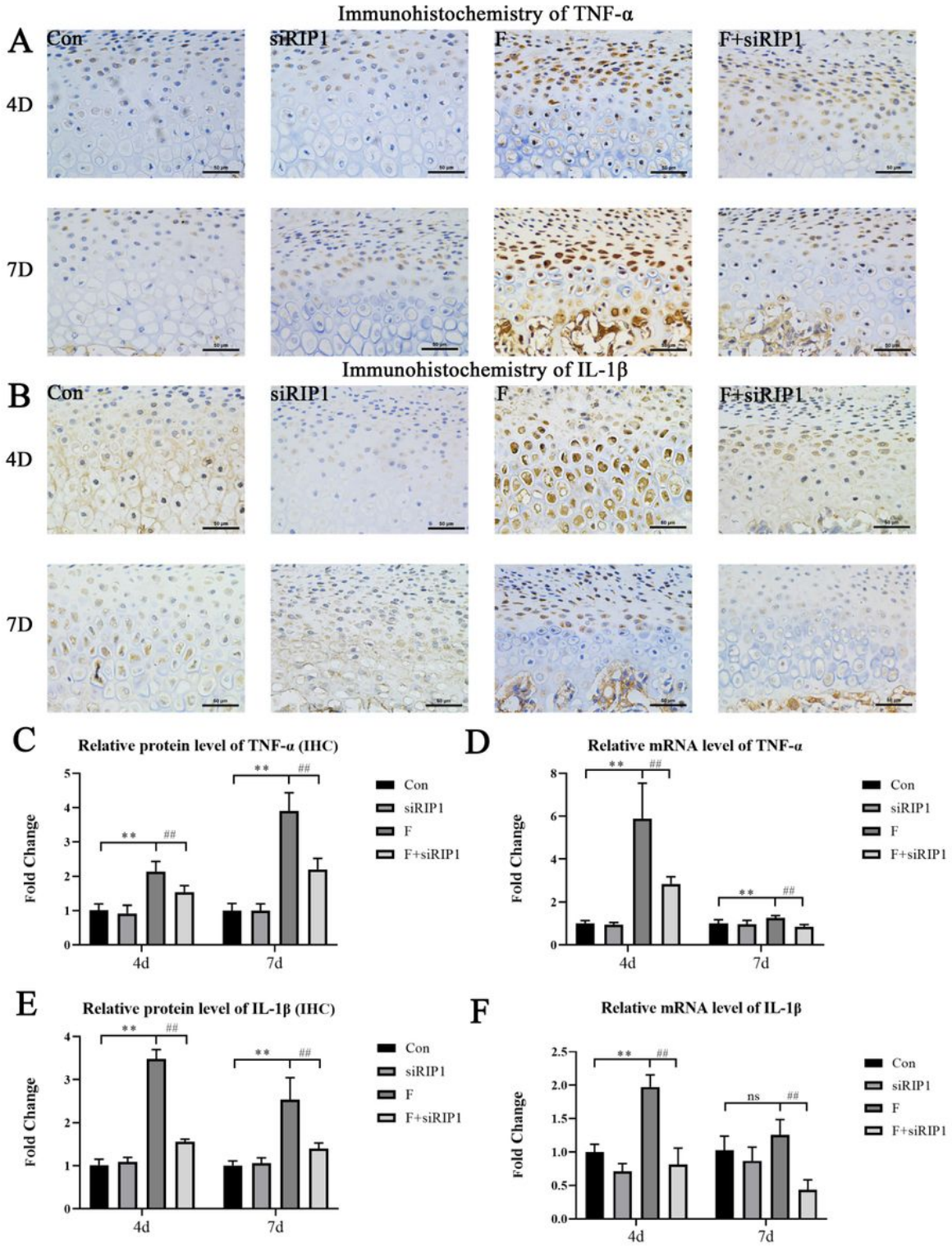

Figure 5

Inflammation of condylar cartilage under mechanical stress was inhibited by Lenti-siRIP1

Condyles from Con, siRIP1, F and F+siRIP1 groups were collected for analysis of relative TNF-α and IL-1β levels. **(a&c)** Immunohistochemical analysis of TNF-α at 4 d and 7 d (n=6). **(b&e)** Immunohistochemical analysis of IL-1β at 4 d and 7 d (n=6). **(d&f)** Relative expression of TNF-α and IL-1β determined by quantitative real-time PCR (n=6). Data were expressed as mean ± SD. (**P*<0.05 vs Con group; ***P*<0.01 vs Con group; #*P*<0.05 vs F group; ##*P*<0.01 vs F group; ns=no significant)

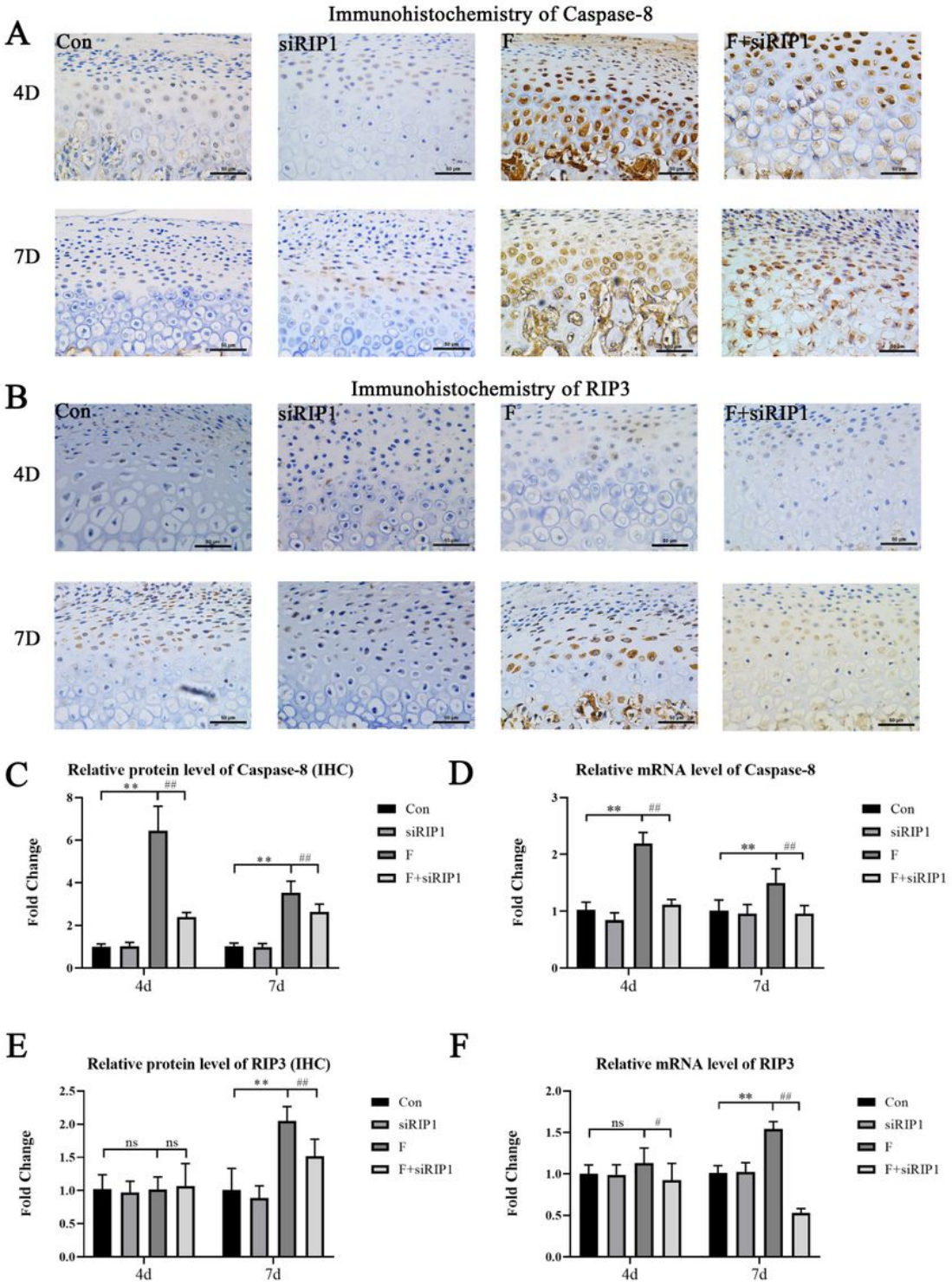

Figure 6

Apoptosis and necroptosis of condylar chondrocytes under mechanical stress were inhibited by Lenti-siRIP1

Condyles from Con, siRIP1, F and F+siRIP1 groups were collected for analysis of relative RIP3 and Caspase-8 levels. **(a&c)** Immunohistochemical analysis of RIP3 at 4 d and 7 d (n=6). **(b&e)** Immunohistochemical analysis of Caspase-8 at 4 d and 7 d (n=6). **(d&f)** Relative expression of RIP3 and Caspase-8 determined by quantitative real-time PCR (n=6). Data were expressed as mean ± SD. (**P*□0.05 vs Con group; ***P*□0.01 vs Con group; #*P*□0.05 vs F group; ##*P*□0.01 vs F group; ns=no significant)

Supplementary Files

This is a list of supplementary files associated with this preprint. Click to download.

- additionalinformation.pdf